Journal of Hepatocellular Carcinoma

Dovepress
Taylor & Francis Group

Open Access Full Text Article

ORIGINAL RESEARCH

Study on the Mechanism of QRICH1 Mediating PRMT1 to Regulate the Arginine Methylation Modification of cGAS to Promote Arsenics-Induced Pyroptosis in Hepatocellular Carcinoma Cells

Jiayuan Zhang[1,2,*], Tian Tian[3,*], Shanshan Tian[1,2], Jinhai Yao[1,2], Yingwan Zhang[4], Rujia Xie[1,2], Ting Yang[1,2], Bing Han[1,2]

[1]Department of Pathophysiology, College of Basic Medical Sciences, Guizhou Medical University, Guiyang, Guizhou, People's Republic of China; [2]Guizhou Provincial Key Laboratory of Pathogenesis and Drug Research on Common Chronic Diseases, Guizhou Medical University, Guiyang, Guizhou, People's Republic of China; [3]Department of Eugenic Genetics, Guiyang Maternal and Child Health Care Hospital, Guiyang, Guizhou, 550003, People's Republic of China; [4]Qianxinan People's Hospital, Qianxinan Affiliated Hospital of Zunyi Medical University, Xingyi, Guizhou, 562400, People's Republic of China

*These authors contributed equally to this work

Correspondence: Bing Han, Email 47569390@qq.com

Purpose: This study aims to investigate the mechanism of action of arsenic-based agents against hepatocellular carcinoma (HCC) and to identify effective drug targets for HCC treatment.

Methods: Huh7 and HepG2 cells treated with NaAsO2 were assessed for cell viability, pyroptosis, migration, and invasion after undergoing lentiviral transfection. An orthotopic liver tumor model was established and divided into a model group and a treatment group. Proteins associated with QRICH1, PRMT1, cGAS-STING, and the classical pyroptosis pathway were quantified using Western blotting. The intracellular expression and localization of PRMT1 and NLRP3 in HCC were analyzed through cellular immunofluorescence. Co-immunoprecipitation (Co-IP) was performed to examine the protein interactions between PRMT1 and cGAS, as well as between STING and NLRP3. Chromatin immunoprecipitation (ChIP) was used to confirm QRICH1 enrichment in the PRMT1 promoter region.

Results: NaAsO2 treatment significantly inhibited the proliferation of Huh7 and HepG2 cells and effectively blocked their migration and invasion capabilities, while promoting cellular pyroptosis. Quantitative polymerase chain reaction(QRCR) and ChIP assays confirmed that NaAsO2 regulates PRMT1 expression by down-regulate QRICH1 binding in the PRMT1 promoter region. Additionally, NaAsO2 decreased the expression of the QRICH1-PRMT1 complex and upregulated the cGAS-STING signaling pathway, activating the downstream NLRP3-dependent classical pyroptosis pathway. Overexpression of QRICH1 reversed these effects.

Conclusion: NaAsO2 inhibits the expression of the QRICH1-PRMT1 axis, activates cGAS-STING signaling pathway transduction, and induces pyroptosis in HCC cells, thereby increasing the infiltration of immune cells in liver cancer tissues.

Keywords: HCC, QRICH1, PRMT1, cGAS-STING, pyroptosis, NaAsO2

Introduction

Hepatocellular carcinoma (HCC) is one of the leading causes of cancer-related deaths worldwide.[1–3] While surgical treatment is the standard approach for early-stage liver cancer, many patients are diagnosed with advanced HCC, rendering surgical interventions impractical.[4,5] The introduction of tumor immunotherapy into clinical practice has opened new possibilities for treatment, as it can target and eliminate tumors while causing minimal harm to surrounding healthy tissues.[6] However, the effectiveness of immunotherapy in HCC often falls short of expectations. This issue primarily arises from the tumor microenvironment associated with HCC, which tends to be "cold" resulting in reduced immunogenicity of HCC-derived tumors.[7–9] Consequently, there is a significant need for innovative combination therapy approaches that can enhance the effectiveness of immunotherapy for HCC. One promising strategy is to increase the

Received: 26 November 2024
Accepted: 4 March 2025
Published: 19 March 2025

immunogenicity of HCC tumors. Inducing immunogenic cell death (ICD) through specific therapies or agents can help convert non-immunogenic cells into an immunogenic state.[10–12] Arsenic formulations, which have their roots in traditional Chinese medicine, have a long history of therapeutic application. Since the 1970s, arsenic trioxide has been successfully used to treat patients with acute promyelocytic leukemia (APL) globally. Furthermore, it has been tested in clinical trials for solid tumors, showing encouraging initial results in foundational studies related to liver cancer.[13,14] Scientists have gradually come to understand and validate the influence of arsenic on tumor cell behavior and its potential role in stimulating anti-tumor immunity.[15] The ability of HCC tumor cells to release antigens and enhance the activation of anti-tumor immune responses has become a key and complex issue in immunotherapy research.

Pyroptosis is a regulated form of cell death that is associated with an inflammatory response. It facilitates the release of antigens and activates the body's adaptive immune response against tumors.[16,17] Among the various inflammasomes, NLRP3 is one of the most extensively studied and plays a crucial role in the classical pyroptosis pathway.

Current studies indicate that NLRP3 inflammasome-mediated classical pyroptosis can significantly inhibit the development of HCC. Furthermore, existing literature has reported a correlation between NLRP3 and tumor immunogenicity in HCC.[18] These findings suggest that the NLRP3-mediated classical pyroptosis pathway may be essential in liver cancer treatment by influencing tumor immunogenicity. Therefore, this research aims to elucidate the specific mechanism by which arsenic activates NLRP3 inflammasomes to induce pyroptosis in HCC.

Recent studies have indicated that the cGAS-STING pathway can regulate the signal transduction of NLRP3 inflammasomes. However, this pathway is typically inactive in tumor cells. The mechanisms by which intratumorous cGAS-STING signaling is inhibited, allowing tumors to evade immune surveillance and promote tumorigenesis, remain unclear. Notably, post-translational modification of cGAS can regulate the enzymatic activity of cGAS in immune cells and tumor cells.

Post-translational modifications refer to the alterations of amino acid side chains that regulate the structure and function of proteins following biosynthesis. Methylation is among the most prevalent and critical of these modifications.[19] In recent years, the relationship between protein arginine methylation and cancer progression has become increasingly evident. PRMT1 significantly contributes to post-translational modifications and is overexpressed in various cancer types. The development of inhibitors targeting PRMT1 has opened new avenues for treating solid tumors and hematologic malignancies.[20] Recent studies indicate that the arginine methyltransferase PRMT1 methylates cGAS at the conserved Arg 133 residue, preventing cGAS dimerization and inhibiting cGAS-STING signaling in cancer cells.[21] This finding provides a theoretical basis for PRMT1's role in mediating arginine methylation of cGAS, thereby inhibiting cGAS-STING signaling and exerting anti-tumor effects. Furthermore, it prompts consideration of whether a similar mechanism exists in HCC, potentially influencing its development.

QRICH1 has been shown to play a regulatory role in endogenous cellular stress (ERS), as demonstrated in a 2021 study published in Science.[22] Furthermore, You et al identified QRICH1 as a key protein within the PERK-eIF2α signaling pathway, which mediates apoptosis in the context of ERS.[23] Building on this foundation, the research group targeted QRICH1 to investigate the potential mechanisms of arsenic-mediated apoptosis in HCC. Based on the results of this study, we conclude that QRICH1 significantly promotes apoptosis in HCC induced by arsenic.[24] However, research on the biological functions of QRICH1 in tumorigenesis and progression is still limited, and its role in tumor immunotherapy remains unexplored. While arsenic has shown potential therapeutic effects on solid tumors, including advanced HCC,[25–27] through modulation of QRICH1 expression, further investigations are necessary to determine whether QRICH1-targeted therapies can effectively inhibit cancer cell development, as the underlying mechanisms are still unclear.

Consequently, our study identifies the QRICH1-PRMT1 regulatory axis as a critical factor influencing the efficacy of immune surveillance. We use this as a foundation to investigate how PRMT1 inhibition can facilitate tumor pyroptosis and enhance lymphocyte infiltration and activation within the tumor microenvironment through a cGAS-dependent mechanism. Our findings may offer valuable insights for identifying effective drug targets to combat the development of HCC.

Materials and Methods

Reagents and Antibodies

Sodium arsenite (NaAsO2) was sourced from Shandong West Asia Chemical Industry Co., LTD. in China. RU.521, a selective inhibitor targeting cGAS, was acquired from MedChemExpress, in China. Matrigel was obtained from BD

Biosciences located in San Jose, CA, United States. N-Diethylnitrosamine (DEN) was provided by Shanghai Aladdin Biochemical Technology Co. The Cell Counting Kit-8 (CCK-8) was procured through Solarbio based in Beijing, China, with the Immunoprecipitation Kit being sourced from Diane in Wuhan, China. The Cellular Pyroptosis Detection Kit was supplied by KeyGEN BioTECH in Nanjing, China, while the Pierce Magnetic CHIP Kit was purchased from Thermo in the USA. The antibodies utilized in this research included rabbit anti-QRICH1 from Abcam in Cambridge, UK, rabbit anti-PRMT1 and cGAS from ZEN Biotechnology in Chengdu, China, rabbit anti-STING from Wuhan Proteintech Biotechnology in China, mouse anti-cleaved caspase-1 from Abmart in Shanghai, China, and rabbit anti-GSDMD (NT), NLRP3, and GAPDH from HuaAn Biotechnology in Hangzhou, China. Furthermore, encoding shRNA-QRICH1 and Oe-QRICH1-specific lentiviral vectors were obtained from GENE in Shanghai, China.

HCC Animal Models

Forty 4–6 week old Balb/c male mice were selected, acclimatized, and fed for one week, and then divided into model mice (n=30) and normal control mice (n=10) using the randomized numerical table method. The model mice were injected intraperitoneally with DEN (100 mg/kg) once, followed by 24 injections of CCl4 (dissolved in olive oil) twice a week at 0.5 mL/kg to induce an animal model of HCC. Control mice were injected intraperitoneally with an equal amount of olive oil. This procedure is in accordance with previously published methods.[28] Changes in the body weight of the mice were recorded once a week during the experiment. After 13 weeks, three mice from the model group and three from the control group were randomly selected and euthanized by cervical dislocation. Paraffin sections of the liver were prepared for HE staining to evaluate liver damage and the development of in situ tumors. Upon confirming the formation of in situ tumors in the liver, the model mice were randomly divided into two groups: the model group and the treatment group. Mice in the treatment group (n = 6) received a total of 10 injections of sodium arsenite (NaAsO2), with three injections per week at a dosage of 5 mL/kg administered intraperitoneally. The model animals (n = 6) were treated with an equivalent volume of phosphate-buffered saline (PBS) for the same duration. Following the completion of the drug administration, all mice were sacrificed via cervical dislocation. Liver tissues were harvested from both the model and treatment groups, while normal liver tissues were collected from the control group.

H&E Staining

Freshly excised mouse liver tissues were fixed in 4% paraformaldehyde, dehydrated, and embedded in paraffin. The samples were then sectioned into 4 μm thick slices. Following this process, the sections were stained using an H&E staining kit and subsequently analyzed pathologically.

Immunohistochemistry

Paraffin-embedded liver sections (4 μm) were deparaffinized, and the tissue sections underwent antigen retrieval using citrate buffer. The sections were subsequently immersed in 3% hydrogen peroxide solution, for a duration of 30 min to inhibit endogenous peroxidase activity, followed by blocking with 5% fetal bovine serum for 1 h. The relevant primary antibodies were then incubated overnight at 4°C.The corresponding secondary antibodies were incubated for 2 h at room temperature. The color reagent was prepared according to the DAB color development kit instructions. After the color reaction was halted, the nuclei were counterstained with Hematoxylin staining solution, and the sections were dehydrated and mounted. Finally, the slides were examined and imaged using a standard light microscope (Olympus, Japan) to observe changes in the corresponding indicators.

Cell Culture and Transfection

Human hepatoma cell lines Huh7 and HepG2 were purchased from Shanghai Cell Bank, Chinese Academy of Sciences. Both cell lines were seeded in Dulbecco's modified eagle medium (DMEM) containing 10% fetal bovine serum and 1% penicillin-streptomycin. The cells were cultured at 37 °C in an incubator with 5% CO_2, and the cells were subcultured at 80% to 90% cell density. Huh7 and HepG2 cells were transfected with lentiviral vectors encoding shRNA-QRICH1 and Oe-QRICH1 specific lentiviral vectors, and then the stably transfected clonal cell lines were screened with medium supplemented with 4 μg/mL puromycin.

Cell Counting Kit-8 Assay

The anti-proliferative effects of NaAsO2 were assessed using the Cell Counting Kit-8 (CCK-8) assay. In summary, cells (5×10^3) were seeded into 96-well plates, allowing them a period of 24 h to adhere prior to treatment with NaAsO2. Afterward, the cells were exposed to a range of NaAsO2 concentrations (0, 5, 10, 20, 40, 80, 120, and 160 μmol/L) for a duration of 24 h. Following this exposure, A total of 10 μL of CCK-8 reagent was introduced to every well, followed by incubating the cells for a duration of 2 h. The absorbance was then recorded at 450 nm utilizing a spectrophotometer (BioRad, Hercules, United States). The IC50 value for NaAsO2 was calculated using GraphPad Prism software (version 9.0.0, GraphPad Software, La Jolla, CA, United States).

Wound Healing Assay

A wound healing assay was conducted to evaluate the effect of NaAsO2 on the migration of HCC cells. In this experiment (5×10^3) cells were seeded into 6-well plates and allowed to grow until a confluent monolayer was established. A sterile micropipette tip (200 μL) was then used to create a wound in the cell layer. After treatment with either 0 μmol/L or 40 μmol/L NaAsO2 for a period of 24 h, the HCC cells were observed and photographed using a microscope at 40x magnification.

Transwell Assay

To study cell invasion and migration in vitro, 24-well transwell plates were used, each consisting of upper and lower chambers made from sterile polycarbonate with an 8 μm pore size. In the cell invasion assay, the upper chambers were coated with 200 μL of Matrigel, while this step was not performed for the migration assay. After treating the cells with either 0 μmol/L or 40 μmol/L NaAsO2 for 24 h, the cells that migrated through the pores were stained with crystal violet. These cells were then photographed and quantified at 40x magnification.

Immunofluorescence

The procedure for tissue sections was partially the same as that for immunohistochemical staining, except that tissue sections were permeabilized with 0.5% Triton X-100 before antigen retrieval. The secondary antibodies used were fluorescently labeled secondary antibodies. For cell experiments, the corresponding number of cell slides were placed in 12-well plates, and cells were seeded in the plates at a density of 1×10^4 cells/well. The cells were cultured in the incubator (37°C, 5% CO_2) for 24 h and the corresponding drugs were added to continue the culture 24 h. The cells were permeabilized with 0.5% Triton X-100 for 30 min at room temperature and blocked in 5% fetal bovine serum for 1 h. Next, the corresponding antibodies (200μL/well) were added and incubated overnight at 4°C. The next day, the primary antibody was recovered and the fluorescent secondary antibody was incubated for 1 h at room temperature in the dark. Finally, the slides were taken out and inverted onto the slide, which had been added with about 10 μL anti-fluorescence quench agent (containing DAPI). The slides were observed and photographed by laser confocal microscope (×40).

Flow Cytometry

The pyroptosis data for HCC cells treated with 0 μmol/L or 40 μmol/L NaAsO2 were gathered using standard flow cytometry (NovoCyte, Agilent, Santa Clara, CA, United States). An assay for cellular pyroptosis detection was employed, following the manufacturer's guidelines carefully. In summary, cells were grown in 6-well plates at a density of 1×10^5 cells per well before the NaAsO2 solution was introduced. After the treatment, cells from each group were harvested, washed with cold phosphate-buffered saline (PBS), and then prepared with a binding buffer. Following this, the cells were stained using Annexin V-APC/PI solution, and the results were analyzed quantitatively with the flow cytometer. The statistical analysis of the data was conducted using the proprietary software NovoExpress® 1.4.1.

Western Blot Analysis

Huh7 and HepG2 cells were treated with 0 μmol/L or 40 μmol/L NaAsO2 for 24 h, followed by two washes with pre-cooled PBS. Subsequently, 200 μL of a cell lysate mixture (Solarbio, cell lysate: protease inhibitor ratio of 99:1) was

added and incubated on ice for 15 min. The cell suspension was then collected using a cell spatula and transferred to a 1.5 mL EP tube. Cells were lysed by sonication and centrifuged at 12,000 rpm for 25 min; the precipitate was discarded, and the supernatant was collected. Protein concentration was quantified using the BCA method, and the protein sample was denatured by adding Protein Sampling Buffer and heating at 100°C for 10 min. Standard sodium dodecyl sulfate gel electrophoresis was performed on the total protein extracts, which were subsequently transferred to a polyvinylidene difluoride (PVDF) membrane. The membranes were blocked with 5% skimmed milk for 1.5 h and washed three times for 5 min each with Tris Buffered Saline containing Tween-20 (TBST). They were then stained overnight at 4°C with the corresponding primary antibodies. The following day, the PVDF membranes were washed with TBST and incubated with secondary antibodies for 1 hour at room temperature. The PVDF membranes containing proteins were treated with an enhanced chemiluminescence reagent, and ImageLab software was utilized to observe the protein bands. The developed images were analyzed using Image J for gray value quantification.

Protein Immunoprecipitation

Huh7 cells were treated with 40 μmol/L of NaAsO2 for 24 h. Magnetic beads coated with antibodies against PRMT1 and STING were used to immunoprecipitate proteins from the cell lysates. The resulting precipitates were then analyzed using Western blotting.

Chromatin Immunoprecipitation

Chromatin Immunoprecipitation (ChIP) was performed using Huh7 cells, following established protocols. The cells were treated with either 0 μmol/L (control) or 40 μmol/L of NaAsO2 prior to the ChIP procedure, using a kit from Thermo Fisher Scientific (Waltham, MA, United States). First, the Huh7 cells were cross-linked with 1% formaldehyde, followed by lysis in sodium dodecyl sulfate lysis buffer. The resulting lysate was sonicated and then centrifuged at 9,000 × g to obtain DNA fragments ranging from 200 to 1,000 base pairs. For immunoprecipitation, the following antibodies were used: QRICH1 (1:50), rabbit IgG (1:50), and anti-RNA polymerase II (1:50). Additionally, an input control without antibodies was included in the experiment. Detection of both input DNA and ChIP DNA was carried out using quantitative polymerase chain reaction (qPCR). The primer sequences for the PRMT1 promoter used in ChIP-qPCR were as follows: Forward: 5'-TCAGACAGGGAGCGGGTGCT-3' and Reverse: 5'-AGGGACAACTTTCACGTGTCACT-3'.

Statistical Analysis

GraphPad Prism 8.0 statistical software was employed to analyze the data in this study. Quantitative data are expressed as mean ± standard deviation. T-tests were utilized for comparisons between two groups, while one-way ANOVA was used for assessing differences among multiple groups. P value of less than 0.05 signifies a statistically significant difference in the results.

Results

DEN Induces in vivo Formation of HCC in Mice, While NaAsO2 Treatment Down-Regulates QRICH1 and up-Regulates Pyroptosis Levels, Thereby Increasing Tumor Immunogenicity

During the modeling period, the body weights of the mice were recorded weekly. The results showed that the body weight of the model group decreased compared to that of the normal control group, with observable signs of depression and reduced mobility. In the treatment group, a temporary increase in body weight was noted following the start of drug administration at week 13. However, there was no significant improvement in the mental status or mobility of the mice (Figure 1A).

Histological characteristics of mouse liver and evaluation of hepatic index: Naked eye observations revealed that the livers of the Control group mice appeared reddish, smooth, and had a soft texture. In contrast, the livers of the Model group mice were dark red, with a greasy feel, rough surfaces, noticeable granularity, and a tough texture. The liver index in the Model group was significantly elevated compared to the Control group. Mice in the group administered with 5mg/

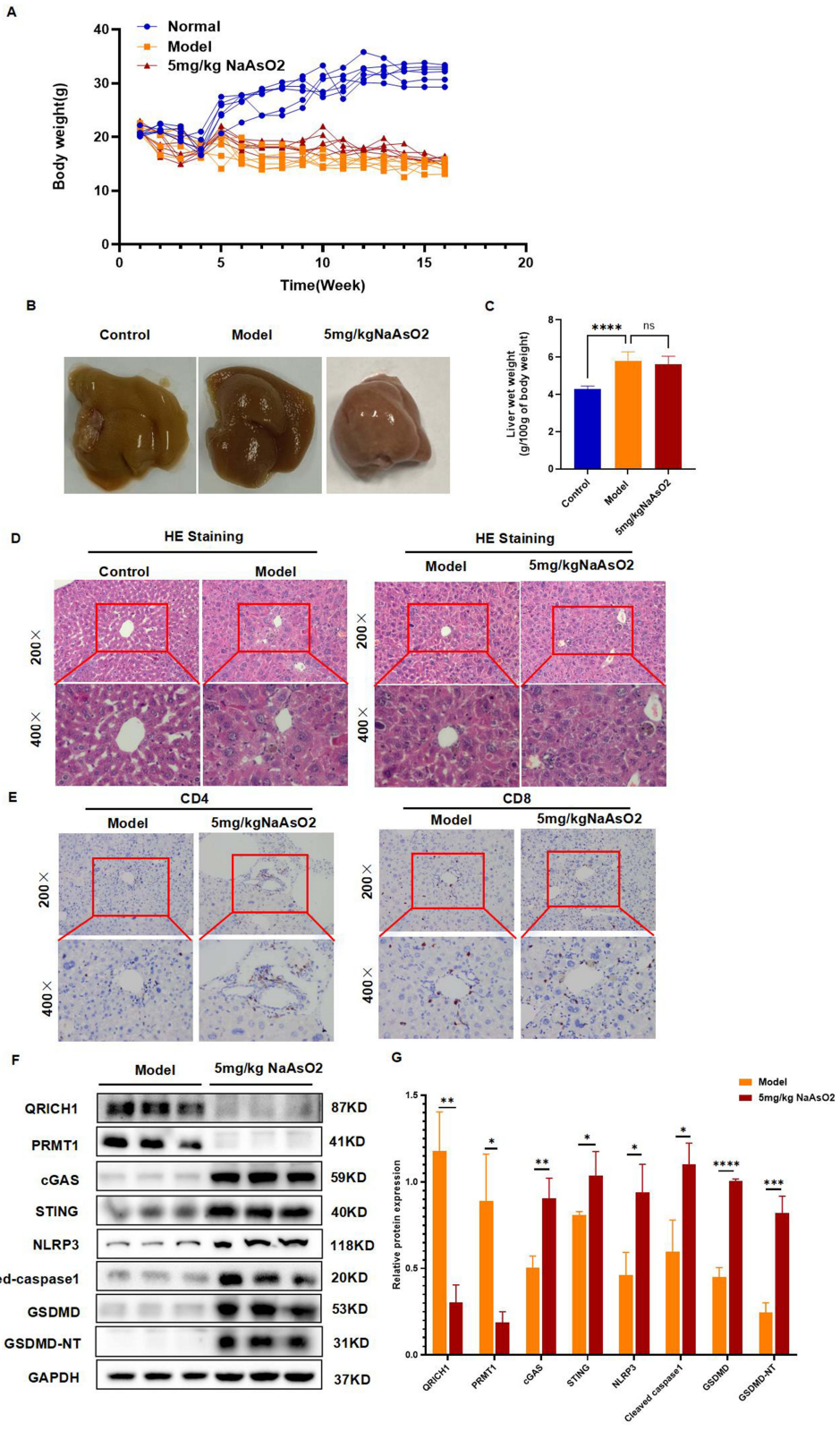

Figure 1 DEN induces in vivo formation of HCC in mice, while NaAsO2 treatment down-regulates QRICH1 and up-regulates pyroptosis levels, thereby increasing tumor immunogenicity. (**A**) Body weight change curve of mice. (**B** and **C**) Histological characterization of mouse liver and evaluation of hepatic indices. Representative images of liver pictures and liver-weight ratios are shown. (**D**) Assessment of liver injury and primary liver cancer progression by H&E staining. Shown are H&E sections and representative images. (**E**) Immunohistochemical staining to detect the expression of CD4+ and CD8+ cells in the liver of mice. Representative IHC stained liver sections. (**F** and **G**) Effect of NaAsO2 on the expression levels of QRICH1, PRMT1, cGAS, STING and pyroptosis-related proteins in HCC as detected by Western blot expression levels in HCC. Representative Western blot images from three independent replicate assays are exhibited. n = 6 animals per experimental group. Data are exhibited as mean ± standard deviation. ns, not significant.
Notes: *P < 0.05, **P <0 0.01, ***P < 0.001, ****P < 0.0001.

kg NaAsO2 had livers that appeared yellowish with diffuse white pitting. The surface roughness of these livers was less pronounced compared to the Model group, The surface roughness of these livers was less pronounced compared to the model group and the liver indices were not significantly different from the model group (Figure 1B and C).Histological examination using HE staining revealed that the liver lobule structure in the normal control group was intact and the hepatocytes were neatly arranged. In contrast, liver tissues from the model group showed disordered arrangements of hepatocytes, along with swelling, degeneration, indistinct cell boundaries, increased cellular heterogeneity, and significantly enlarged nuclei. The histopathological condition of the liver in the treatment group did not differ from that of the model group (Figure 1D). Immunohistochemical analysis demonstrated a significant increase in the infiltration of CD4+ and CD8+ T-cells in the treatment group compared to the model group (Figure 1E).

Western blot analysis indicated that the expression levels of QRICH1 and PRMT1 in liver tissues were reduced in the treatment group relative to the model group. In contrast, the expression of cGAS-STING and proteins associated with the classical pyroptosis pathway was elevated (Figure 1F and G). In summary, an in situ HCC model in mice was successfully established using DEN in combination with CCl4. Treatment with NaAsO2 enhanced the immune infiltration of CD4+ and CD8+ lymphocytes within the HCC tissues and induced pyroptosis in mouse HCC cells. We speculate that the increased infiltration of immune cells, which may effectively combat the progression of HCC following NaAsO2 treatment, is associated with the downregulation of QRICH1 and the upregulation of cGAS-STING and pyroptosis-related proteins.

NaAsO2 Suppresses HCC Cell Growth

In previous studies conducted by our group, we demonstrated that NaAsO2 inhibits the overgrowth of HepG2 cells and induces apoptosis via QRICH1. To further elucidate the mechanism by which NaAsO2 impedes HCC development, we treated HCC cell lines Huh7 and HepG2 with varying concentrations of NaAsO2 for 24 h. The CCK-8 assay for cell proliferation revealed that the growth of NaAsO2-treated HCC cells was significantly inhibited (Figure 2A), with an IC50 of 40 μmol/L. Therefore, NaAsO2 at a final concentration of 40 μmol/L was selected for subsequent experiments, maintaining an exposure time of 24 h. In wound healing, migration, and transwell assays, NaAsO2 reduced the migration and invasion capabilities of HCC cells in vitro (Figure 2B–D). Furthermore, Western blot analysis indicated that NaAsO2 downregulated the protein expression of QRICH1 and PRMT1 in HCC cells, while also upregulating the expression levels of cGAS, STING, and proteins associated with the classical pyroptosis pathway (Figure 2E and F). These findings suggest that NaAsO2 downregulates QRICH1 and modulates the cGAS-STING pathway, leading to the activation of the classical pyroptosis pathway.

Interaction Between PRMT1 and cGAS, STING, and NLRP3 in HCC Cells

In Huh7 cells, chromatin immunoprecipitation (ChIP) assays revealed that treatment with NaAsO2 resulted in a decreased level of QRICH1 enrichment in the promoter region of PRMT1 (Figure 3A). Co-immunoprecipitation (Co-IP) analysis further illustrated the complex protein interactions among QRICH1, PRMT1, cGAS, STING, and NLRP3 in HCC cells. This analysis showed direct interactions between QRICH1 and PRMT1, as well as between PRMT1 and the proteins cGAS, STING, and NLRP3 (Figure 3B). To explore the relationship between pyroptosis and the cGAS-STING signaling pathway further, HCC cells were treated with the cGAS inhibitor RU.521 (1 μmol/L). The resulting data demonstrated a significant reduction in the expression levels of cGAS and STING proteins in HCC, along with a notable decrease in the levels of proteins associated with the classical pyroptosis pathway (Figure 3C–F). Our results suggest that the inhibition of cGAS effectively reverses the NLRP3-dependent classical pyroptosis triggered by NaAsO2 in HCC. In summary, NaAsO2 induces pyroptosis in HCC cells by suppressing the QRICH1-PRMT1 axis, which in turn influences the cGAS-STING signaling pathway.

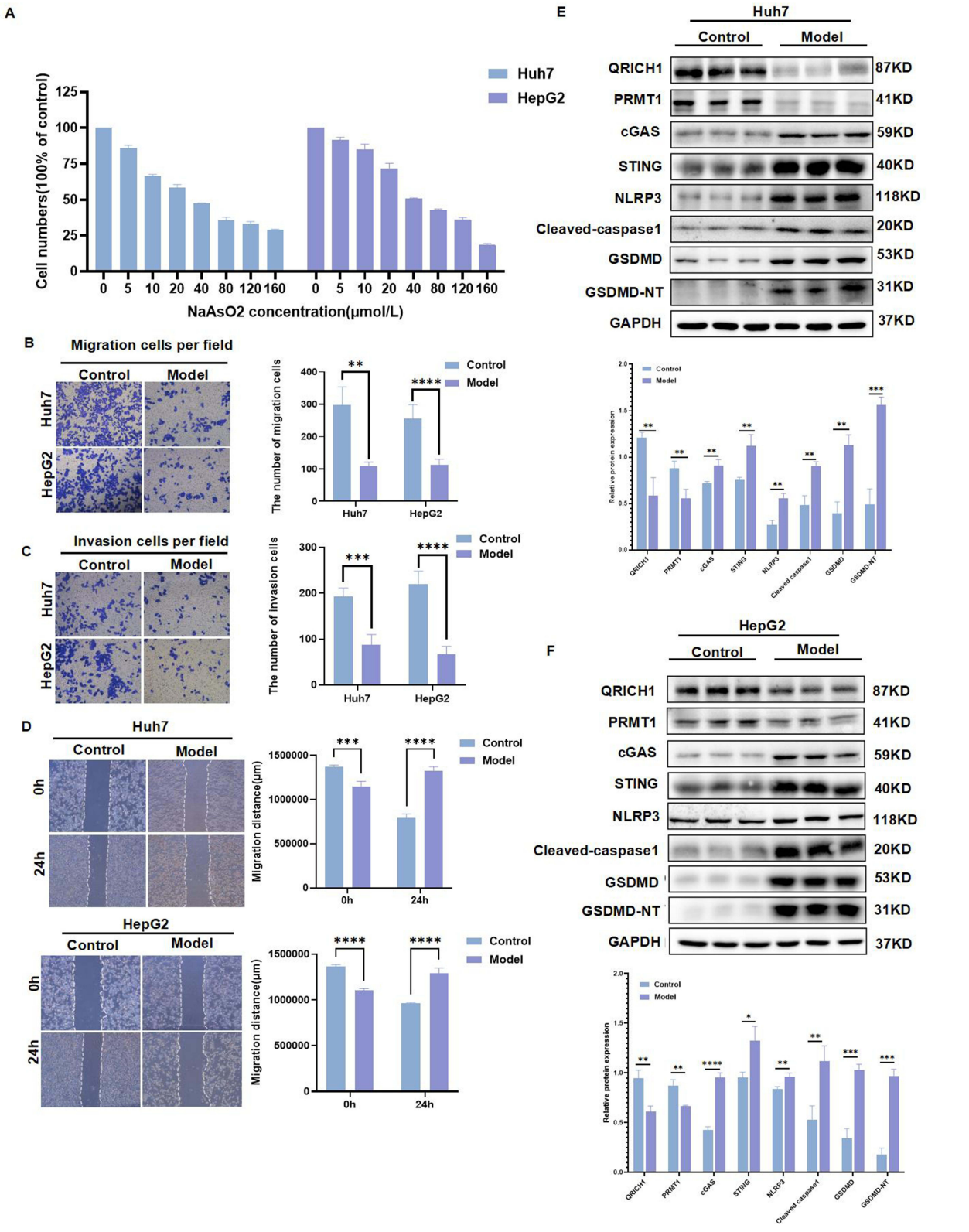

Figure 2 NaAsO2 suppresses HCC cell growth. (**A**) The proliferation of Huh7 and HepG2 cells following NaAsO2 treatment was assessed using the CCK8 assay. Experiments were repeated thrice. Representative results from three independent replicate assays are shown. (**B–D**) The effects of NaAsO2 treatment on migration, invasion and scratch healing in Huh7 and HepG2 cells were verified. Representative pictures of invaded HCC cells from three independent replicate assays are exhibited. All cells were observed under an inverted microscope with a 40-fold objective lens. (**E** and **F**) Western blotting was employed to examine the expression of the QRICH1-PRMT1 axis, the cGAS-STING signaling pathway, and classical pyroptosis-related proteins. Representative Western blot images from three independent replicate assays are exhibited. Data are exhibited as mean ± standard deviation.
Notes: *P < 0.05, **P <0.01, ***P < 0.001, ****P < 0.0001.

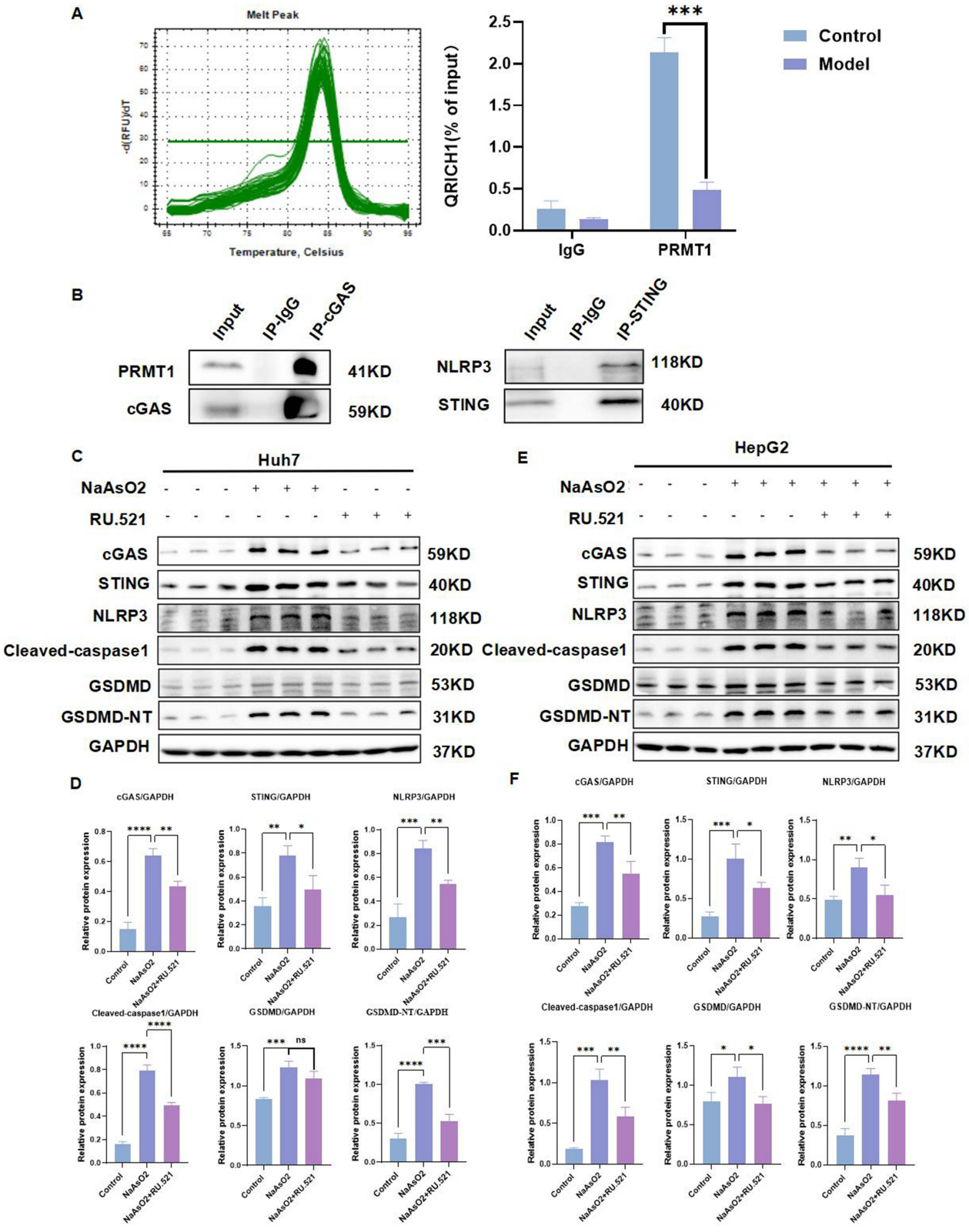

Figure 3 Interaction between PRMT1 and cGAS, STING, and NLRP3 in HCC Cells. (**A**) Displays the assessment of QRICH1 enrichment within the promoter region associated with PRMT1 in Huh7 cells subjected to NaAsO2 treatment, evaluated through chromatin immunoprecipitation coupled with quantitative polymerase chain reaction. (**B**) Examines the interactions between PRMT1, cGAS, STING, and NLRP3 in Huh7 cells treated with sodium arsenite, employing protein immunoprecipitation alongside Western blot analysis. (**C–F**) Investigate the levels of proteins linked to the cGAS-STING signaling pathway and classical pyroptosis pathway utilizing Western blotting. Representative Western blot images from three independent replicate assays are exhibited. Data presents as mean ± standard deviation with three replicates. ns, not significant.

Notes: *P < 0.05, **P < 0.01,***P < 0.001, ****P < 0.0001.

https://doi.org/10.2147/JHC.S505266

The Expression Regulation of QRICH1 Affects NaAsO2's Inhibitory Impact on the Migration and Invasion of HCC

To further clarify the function of QRICH1 in the process of NaAsO2-induced pyroptosis, we initially transfected Huh7 and HepG2 cells using lentiviral vectors that carried QRICH1-specific shRNA and Oe-QRICH1, respectively. After a 72 h incubation, green fluorescence was visualized through fluorescence microscopy (Figure 4A), and the transfection efficiency was evaluated by Western blot analysis (Figure 4B). The findings revealed a significant reduction in QRICH1 expression in HCC cells that received sh-QRICH1 transfection, while a notable increase was observed in HCC cells transfected with Oe-QRICH1. Both Huh7 and HepG2 cells underwent the same treatment (40 μmol/L NaAsO2). During the migration and Transwell invasion assays, cells in the QRICH1 silencing group demonstrated an intensified inhibition of HCC cell migration and invasion triggered by NaAsO2, whereas a contrasting effect was detected in the QRICH1 overexpression group (Figure 4C and D). These results indicate that decreased QRICH1 levels can hinder the migration, and invasion of HCC cells, while the overexpression of QRICH1 may partially alleviate the inhibitory effects of NaAsO2 on HCC cell migration, and invasion.

Knockdown of QRICH1 Activated the cGAS-STING Signaling Axis in HCC, While Overexpression of QRICH1 Partially Reversed This Effect

The levels of QRICH1, PRMT1, cGAS, and STING proteins were assessed using Western blot analysis. The results showed a decrease in QRICH1 and PRMT1 protein levels, along with an increase in cGAS and STING protein levels in the knockdown group (Figure 5A and B). In contrast, the opposite trend was observed in HepG2 cells that overexpressed QRICH1 (Figure 5C and D). Changes in PRMT1 protein expression (red) were further confirmed through immunofluorescence (Figure 5E and F). These findings indicate that QRICH1 knockdown downregulates the expression of PRMT1 in HCC cells while simultaneously activating the cGAS-STING signaling pathway. Notably, overexpression of QRICH1 mitigated the effects induced by NaAsO2 to some extent.

Knockdown of QRICH1 Exacerbated Pyroptosis in HCC, While Overexpression of QRICH1 Effectively Reduced NaAsO2-Induced Pyroptosis in HCC Cells

Flow cytometry analysis demonstrated that knocking down QRICH1 promoted NaAsO2-induced pyroptosis in Huh7 cells. Conversely, an opposite effect was observed in the QRICH1 overexpression group (Figure 6A). Subsequently, classical pyroptosis-related proteins were analyzed using Western blot, revealing a increased in these protein levels in the knockdown group. In contrast, decrease levels of pyroptosis-related proteins were detected in HepG2 cells that overexpressed QRICH1 (Figures 6B–E). These changes in NLRP3 protein expression (red) were further confirmed through immunofluorescence (Figure 6F and G). These data suggest that a reduction in QRICH1 levels can activate the classical NLRP3-dependent pyroptosis pathway, whereas QRICH1 overexpression can mitigate NaAsO2-induced pyroptosis to some extent.

Discussion

Liver cancer, ranked among the top eight most common cancers globally, is characterized by its aggressive nature and high propensity for recurrence and metastasis, contributing to over 60% of newly diagnosed cancer cases and cancer-related deaths. HCC is the predominant form of liver cancer and a leading cause of cancer mortality.[29] Despite the availability of various treatment options for early-stage HCC, many patients receive their diagnosis at more advanced stages, leading to a reduced selection of treatments and a grim prognosis.[30] While arsenic has shown initial promise in treating solid tumors, whether used alone or in conjunction with other therapies, its effectiveness in addressing liver cancer remains limited.[31,32]

Recently, immunotherapy has emerged as a rapidly evolving tactic for managing advanced HCC.[6] Accumulating evidence indicates that the innate immune system plays a crucial role in immune surveillance and the efficacy of immunotherapy for liver cancer.[33] The predominant tumor-infiltrating lymphocytes within the tumor microenvironment (TME) include CD4+ T helper cells and effector CD8+ T cells, with CD8+ T cells, in particular, being pivotal in the elimination of malignant cancer

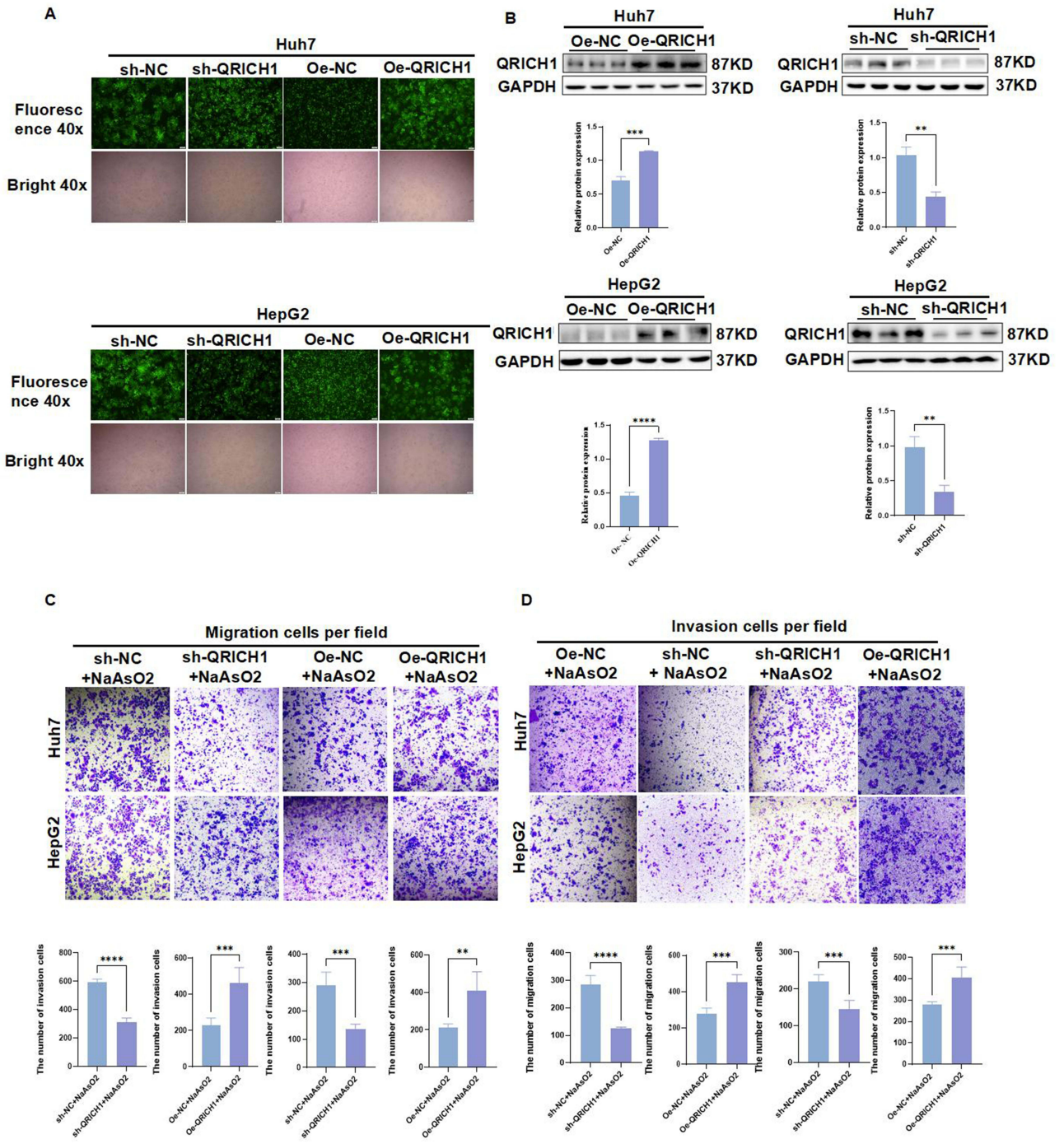

Figure 4 The expression regulation of QRICH1 affects NaAsO2's inhibitory impact on the migration and invasion of HCC. (**A**) Lentivirus encoding QRICH1-specific shRNA and Oe-QRICH1 was used to transfect the Huh7 and HepG2 cell lines, with green fluorescence observed through fluorescence microscopy 48 to 72 h after transfection. All cells were observed under an inverted microscope with a 40-fold objective lens. (**B**) Western blot analysis was utilized to evaluate the effects of QRICH1 overexpression in Huh7 and HepG2 cells, alongside the outcomes of QRICH1 inhibition. Representative Western blot images from three independent replicate assays are exhibited. (**C**) Transwell assay was performed to determine the migration capabilities of the cells. (**D**) Transwell assay was conducted to assess the invasion capacities of the cells. For panel (**C** and **D**) Representative pictures of invaded HCC cells from three independent replicate assays are exhibited. Data presents as mean ± standard deviation with three replicates.

Notes: **P < 0.01, ***P < 0.001, ****P < 0.0001.

cells.[34] The infiltration of immune cells into the TME is essential for the strength of the body's anti-tumor immune response; however, low immunogenicity remains a central challenge that hinders the advancement of tumor immunotherapy. Theoretically, human cancers can be classified into two primary types: "hot" and "cold" tumors. "Cold" tumors show minimal

https://doi.org/10.2147/JHC.S505266

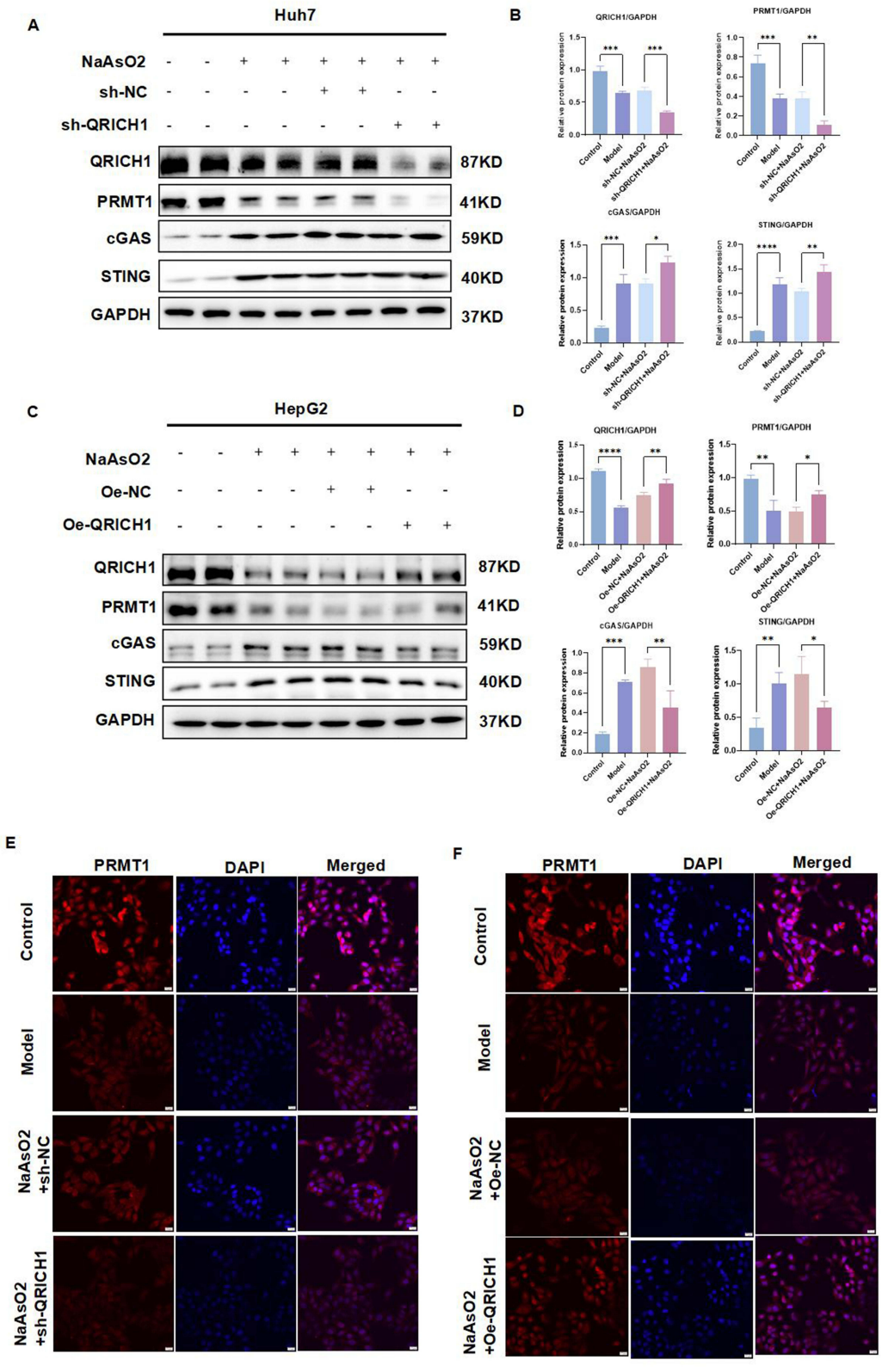

Figure 5 Knockdown of QRICH1 activated the cGAS-STING signaling axis in HCC, while QRICH1 overexpression partially reversed this effect. (**A**–**D**) Protein levels of QRICH1, PRMT1, cGAS, and STING in cells were determined by Western blot. Representative Western blot images from three independent replicate assays are exhibited. (**E** and **F**) PRMT1 expression was measured using laser confocal technique. The cells were observed under a confocal microscope (×400 magnification). Data presents as mean ± standard deviation with three replicates.

Notes: *P < 0.05, **P < 0.01, ***P < 0.001, ****P < 0.0001.

immune cell infiltration and are typically resistant to immune checkpoint inhibitors (ICIs).[35,36] Recent investigations have increasingly shown that arsenic agents might trigger immunogenic cell death in tumor cells.[37] This phenomenon involves a series of molecular processes, beginning with the extracellular release of immunostimulatory factors by tumor cells, such as

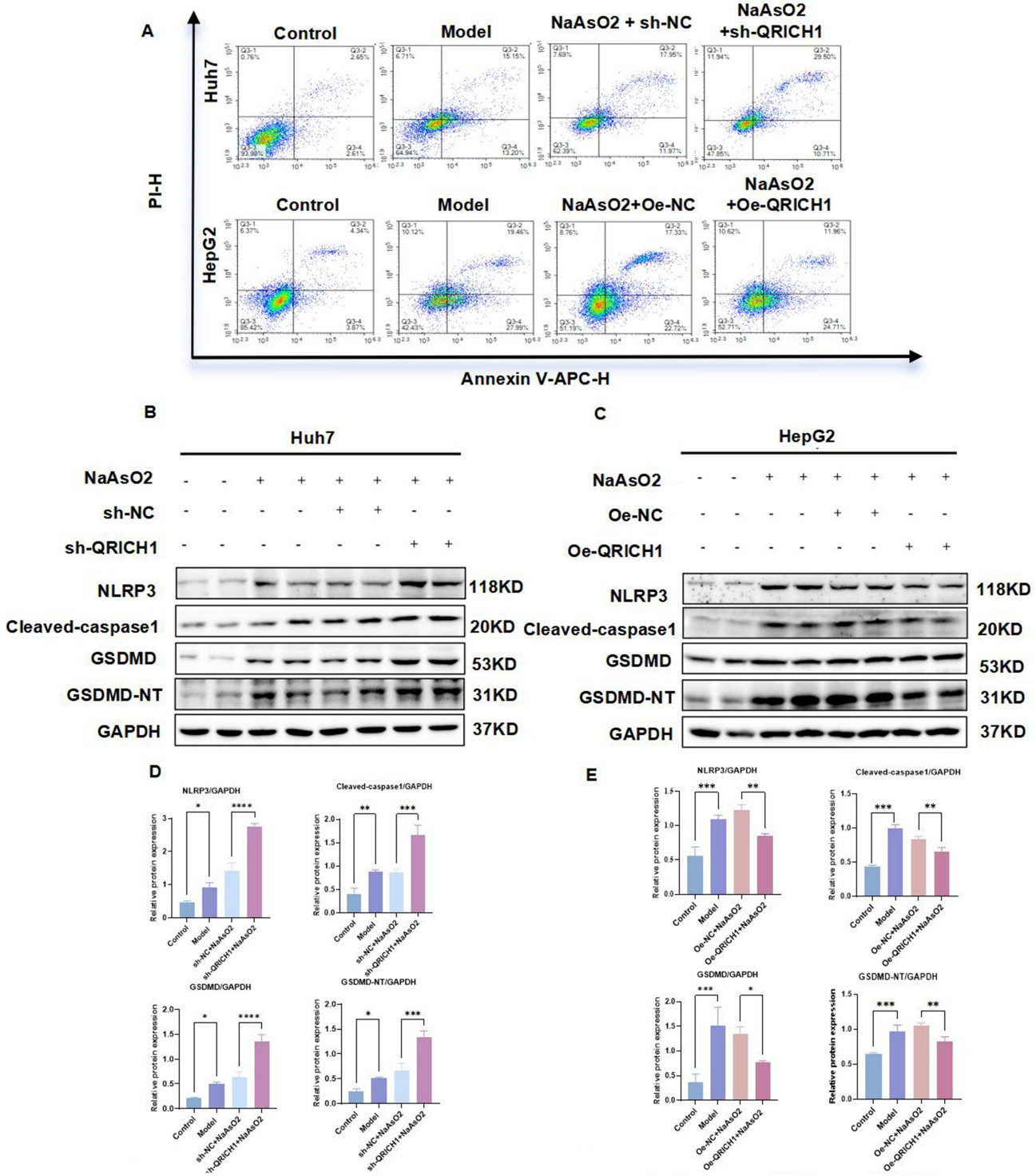

Figure 6 Continued.

https://doi.org/10.2147/JHC.S505266

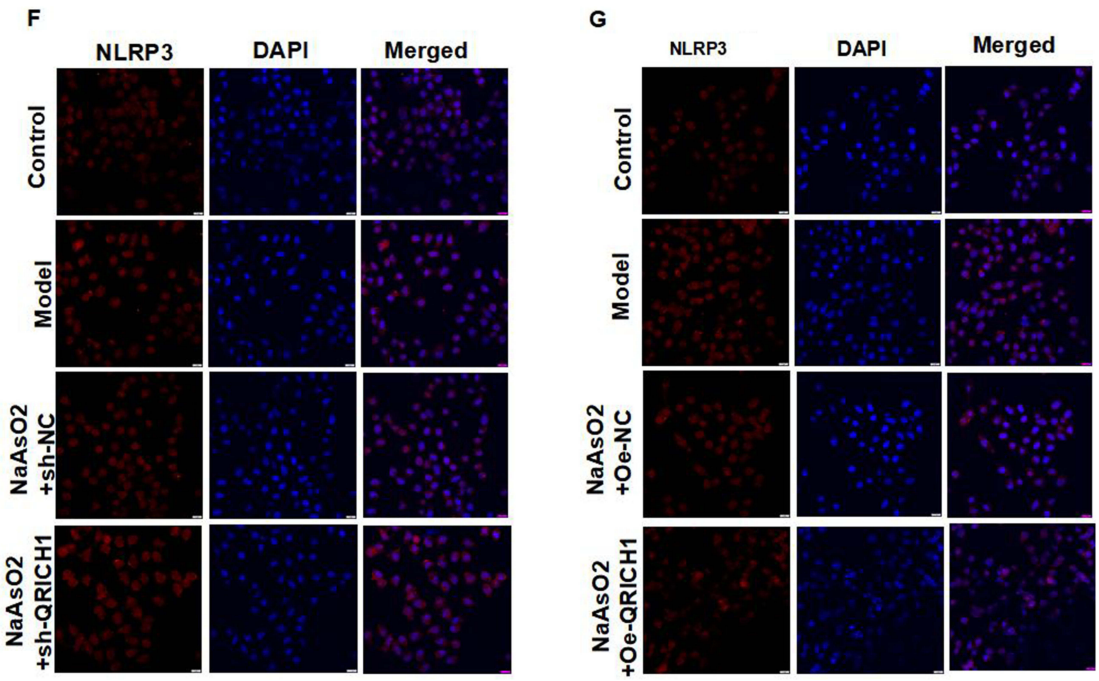

Figure 6 Knockdown of QRICH1 exacerbated pyroptosis in HCC, while overexpression of QRICH1 effectively reduced NaAsO2-induced pyroptosis in HCC cells. (**A**) Double staining of cells was assessed using flow cytometry. Representative pictures from three independent replicate assays are exhibited. (**B**–**E**) The protein levels of classical pyroptosis-related in the cells were analyzed by Western blot. Representative Western blot images from three independent replicate assays are exhibited. (**F** and **G**) NLRP3 expression was evaluated using laser confocal microscopy. The cells were observed under a confocal microscope (×400 magnification). The scale is 20 μm; Data presents as mean ± standard deviation.

Notes: *P < 0.05, **P < 0.01, ***P < 0.001, ****P < 0.0001.

Abbreviation: PI: Propidium iodide.

adenosine triphosphate (ATP), DAMPs, high-mobility group box 1 (HMGB1), and inflammatory mediators play a crucial role in immune responses. When these immunostimulatory components are released, they are recognized by pattern recognition receptors (PRRs) present on antigen-presenting cells, including macrophages and dendritic cells (DCs). This recognition enables the presentation of these factors on their surfaces, thereby enhancing the body's anti-tumor immune mechanisms. Currently, a variety of therapeutic approaches are employed alongside immune checkpoint inhibitors (ICIs) to enhance the attraction of immune cells and convert "cold" tumors into "hot" tumors.[36,38–40]

Pyroptosis is a distinct form of inflammatory programmed cell death characterized by the activation of caspases, the cleavage of gasdermin (GSDM), the disruption of cellular membranes, and the rapid release of DAMPs along with pro-inflammatory cytokines.[41–43] Research indicates that the significant release of DAMPs and pro-inflammatory cytokines resulting from pyroptosis effectively stimulates the immune response.[44] Among the various pathways involved in pyroptosis, the classical pyroptosis pathway has garnered the most attention. In this regard, the NLRP3 inflammasome, one of the most extensively researched inflammasomes, is vital. Recent investigations have revealed that activating NLRP3 inflammasome-mediated pyroptosis can considerably hinder the progression of HCC. Moreover, it has been observed that the components of the NLRP3 inflammasome are markedly downregulated in HCC cells, leading to a reduction in the pyroptosis process within HCC cells and tissues.[18]

Taking this into account, it is crucial to pursue additional research regarding the influence of the NLRP3 inflammasome on HCC progression. The way in which the NLRP3 inflammasome-GSDMD axis regulates the pyroptosis pathway presents a novel strategy for enhancing the efficacy of immunotherapy. In this context, the NLRP3 inflammasome serves as a vital molecular detector that identifies inflammatory signals within the organism. When activated, it leads to the release of cytokines IL-1β and IL-18 through GSDMD cleavage, which subsequently forms pores in the cell membrane and initiates pyroptosis.[45] This mechanism significantly affects tumor development and progression. Therefore, gaining a more profound understanding of the unique roles played by the NLRP3 inflammasome and GSDMD-mediated pyroptosis

in HCC is essential for elucidating the mechanisms behind tumorigenesis and for creating targeted therapeutic strategies. Our research revealed that NaAsO2 increased the infiltration of cytotoxic T lymphocytes (CTLs) in primary HCC samples. In vitro experiments further confirmed that NaAsO2 treatment effectively restrained the proliferation, migration, and invasion of HCC cells. Notably, we observed that NaAsO2 could provoke pyroptosis in HCC cells both in vivo and in vitro, which supports our initial hypothesis. These findings offer new insights into the ways in which NaAsO2 influences HCC treatment.

Protein post-translational modifications (PTMs) are critical for enhancing proteome diversity and sustaining cellular homeostasis. Among these modifications, arginine methylation, which remains underexplored, has garnered significant attention in recent years. As research progresses, accumulating evidence suggests a close relationship between arginine methylation and cancer progression. A deeper understanding of the epigenetic regulatory role of arginine methylation in disease initiation and progression has paved the way for new strategies in drug discovery and targeted therapy. Among the various arginine methyltransferases, PRMT1, the most prominent member in mammals, has rapidly emerged as a focal point of research. However, the intricate nature of arginine methylation means that the mechanisms underlying the potential therapeutic benefits of PRMT1 inhibition are not yet fully understood. Recent studies suggest that PRMT1 is involved in the methylation of cGAS-STING in cancer cells, with PRMT1 directly methylating cGAS and consequently suppressing cGAS-STING signaling, which facilitates immune evasion in tumors. This finding lays a theoretical groundwork for evaluating PRMT1 as a possible target in immunotherapy.

Considering that PRMT1-mediated methylation partially suppresses the basal activity of the cGAS-STING signaling pathway in tumors, inhibiting PRMT1 is expected to improve the immunogenicity within the TME of cancer patients. To further elucidate the regulatory relationship between PRMT1 and the cGAS-STING pathway, as well as pyroptosis in HCC, we confirmed the protein interactions among PRMT1, cGAS, STING, and NLRP3 using a Co-IP assay. Subsequently, we treated HCC cells with the cGAS inhibitor RU.521, and the results aligned with our expectations: RU.521 diminished sodium arsenite-induced pyroptosis in HCC, with its effect positively correlated with the activation of the cGAS-STING pathway.

In summary, our definition of the PRMT1-cGAS-STING signaling axis offers a novel perspective on how the inhibition of PRMT1 activates the cGAS-STING signaling pathway and its downstream associated molecules. This mechanism suggests that the activation of pyroptosis may initiate an anti-tumor immune response, thereby presenting new ideas and potential targets for the treatment of HCC.

In a prior investigation, we demonstrated that sodium arsenite can promote apoptosis and inhibit the growth of HCC by downregulating the protein level of QRICH1 and initiating the apoptosis pathway associated with endoplasmic reticulum stress.[24] In the current research, we discovered that sodium arsenite can showcase a tumor-suppressive effect by reducing the expression of QRICH1 in HCC. QRICH1, which is a transcription factor featuring a CARD domain, has gained considerable attention recently and plays a crucial regulatory role in the signaling pathway associated with endoplasmic reticulum stress. We affirmed the direct regulatory connection between QRICH1 and PRMT1 through ChIP assays. Hence, we suggest a potential mechanism regarding the down-regulation of QRICH1 following treatment with arsenite in HCC; this process would lead to the demethylation of PRMT1 on cGAS, subsequently activating the cGAS-STING pathway, thus triggering the NLRP3 inflammasome activation, while also enhancing the infiltration and functional efficacy of cytotoxic T lymphocytes. To validate this hypothesis, we created stably transfected cloned cell lines employing lentiviral vectors that encode shRNA-QRICH1 (sh-QRICH1) and overexpress QRICH1 (Oe-QRICH1). The findings indicated that the down-regulation of QRICH1 expression could stimulate the cGAS-STING signaling pathway by inhibiting PRMT1 and promote pyroptosis in HCC, while the increase in QRICH1 expression could partially reverse this effect.

In this study, we found that sodium arsenite can exert a tumor suppressive effect by inhibiting QRICH1 expression in HCC. QRICH1, a transcription factor with a CARD domain, has received much attention in recent years and plays an important regulatory role in the ERS signaling pathway. We verified the direct regulatory relationship between QRICH1 and PRMT1 through ChIP experiments. Therefore, we propose a potential mechanism of QRICH1 down-regulation after treatment with arsenide on HCC, which will eliminate the methylation of PRMT1 on cGAS, activate the cGAS-STING pathway, and then induce the activation of NLRP3 inflammasome, while enhancing the infiltration and effector function of cytotoxic T lymphocytes. To confirm this hypothesis, we constructed stable transfected cloned cell lines using lentiviral vectors encoding shRNA-QRICH1 and Oe-QRICH1. The results showed that down-regulation of QRICH1 expression could activate the cGAS-STING

signaling pathway by inhibiting PRMT1 and induce pyroptosis of HCC, while up-regulation of QRICH1 expression could reverse this trend to some extent.

In conclusion, we propose a mechanism through which NaAsO2 inhibits the expression of QRICH1, regulates the activation of the PRMT1-mediated cGAS-STING pathway, induces pyroptosis in HCC cells, and enhances the immunogenicity of the HCC tumor microenvironment, thereby inhibiting HCC. Our findings underscore that targeting QRICH1 may represent an effective strategy to slow HCC progression and immune evasion, thereby offering new avenues for cancer immunotherapy.

Conclusion

NaAsO2 reduces PRMT1 expression via the down-regulation of QRICH1, which diminishes the methylation of cGAS and facilitates the activation of the cGAS-STING pathway. This results in pyroptosis in HCC and enhances the immunogenicity of HCC, fostering cell death in HCC.

Institutional Review Board Statement

All experimental procedures involving animals were conducted in full compliance with the Guide for the Care and Use of Laboratory Animals (NIH Publication No. 85-23, revised 1996) and received approval from the Laboratory Animal Center at Guizhou Medical University (Guizhou, China). The assigned approval number:NO 2400576.

Data Sharing Statement

All data are available upon request from the correspondence author.

Author Contributions

All authors made a significant contribution to the work reported, whether that is in the conception, study design, execution, acquisition of data, analysis and interpretation, or in all these areas; took part in drafting, revising or critically reviewing the article; gave final approval of the version to be published; have agreed on the journal to which the article has been submitted; and agree to be accountable for all aspects of the work.

Funding

The authors have acknowledged the financial assistance received for the research, authorship, and/or publication of this article as follows: This study received funding from the National Natural Science Foundation of China (Grants No. 81100284 and 82260127), the Guizhou Science and Technology Cooperation Platform Personnel [2018] (Grant No. 5779-19), the Science and Technology Foundation of Guizhou Province (Qiankehe Jichu-ZK [2021] 364, Qiankehe Jichu-ZK [2021] 365 and Qiankehe Jichu-MS [2025] 544), as well as the Cultivation Project of the National Natural Science Foundation at Guizhou Medical University 20NSP003.

Disclosure

The authors declare that there is no competing interest in this work.

References

1. Bray F, Laversanne M, Sung H, et al. Global cancer statistics 2022: GLOBOCAN estimates of incidence and mortality worldwide for 36 cancers in 185 countries. *Ca a Cancer J Clin*. 2024;74(3):229–263. doi:10.3322/caac.21834
2. Oh JH, Jun DW. The latest global burden of liver cancer: a past and present threat. *Clin Mol Hepatol*. 2023;29:355–357. doi:10.3350/cmh.2023.0070
3. Siegel LR, Giaquinto NA, Jemal A. Cancer statistics, 2024. *Ca a Cancer J Clin*. 2024;74(1):12–49. doi:10.3322/caac.21820
4. Allaire M, Bruix J, Korenjak M, et al. What to do about hepatocellular carcinoma: recommendations for health authorities from the international liver cancer association. *JHEP Rep*. 2022;4:100578. doi:10.1016/j.jhepr.2022.100578
5. Liu CY, Cheng CY, Yang SY, et al. Mortality evaluation and life expectancy prediction of patients with hepatocellular carcinoma with data mining. *Healthcare*. 2023;11:925. doi:10.3390/healthcare11060925
6. Callahan KM, Postow AM, Wolchok DJ. Targeting T cell co-receptors for cancer therapy. *Immunity*. 2016;44(5):1069–1078. doi:10.1016/j.immuni.2016.04.023
7. Zhang H, Zhang W, Jiang L, Chen Y. Recent advances in systemic therapy for hepatocellular carcinoma. *Biomark Res*. 2022;10:3. doi:10.1186/s40364-021-00350-4

8. Sangro B, Sarobe P, Hervas-Stubbs S, et al. Advances in immunotherapy for hepatocellular carcinoma. *Nat Rev Gastroenterol Hepatol*. 2021;18:525–543. doi:10.1038/s41575-021-00438-0
9. Donne R, Lujambio A. The liver cancer immune microenvironment: therapeutic implications for hepatocellular carcinoma. *Hepatology*. 2023;77:1773–1796. doi:10.1002/hep.32740
10. Birmpilis AI, Paschalis A, Mourkakis A, et al. Immunogenic cell death, DAMPs and prothymosin alpha as a putative anticancer immune response biomarker. *Cells*. 2022;11:1415. doi:10.3390/cells11091415
11. Rodrigues MC, Morais JAV, Ganassin R, et al. An overview on immunogenic cell death in cancer biology and therapy. *Pharmaceutics*. 2022;14:1564. doi:10.3390/pharmaceutics14081564
12. Cui Y, Li Y, Long S, et al. Comprehensive analysis of the immunogenic cell death-related signature for predicting prognosis and immunotherapy efficiency in patients with lung adenocarcinoma. *BMC Med Genomics*. 2023;16:184. doi:10.1186/s12920-023-01604-w
13. Weizhe Z, Zhuqing R, Jianhua R, et al. Aging aggravated liver ischemia and reperfusion injury by promoting STING-mediated NLRP3 activation in macrophages. *Aging Cell*. 2020;19(8):e13186. doi:10.1111/acel.13186
14. Ke-Zhi Z, Qiang-Bo Z, Quan-Bao Z, et al. Arsenic trioxide induces differentiation of CD133+ hepatocellular carcinoma cells and prolongs posthepatectomy survival by targeting GLI1 expression in a mouse model. *J hematol oncol*. 2014;7(1):28. doi:10.1186/1756-8722-7-28
15. Ji-Zhong Y, Xiao-Qian S, Ming-Dong W, et al. Arsenic trioxide elicits anti-tumor activity by inhibiting polarization of M2-like tumor-associated macrophages via notch signaling pathway in lung adenocarcinoma. *Int Immunopharmacol*. 2023;117:109899. doi:10.1016/j.intimp.2023.109899
16. S MJ, N JM, M EN, et al. GasderminD hypermethylation inhibits pyroptosis and LPS-Induced IL-1beta Release From NK92 cells. *Immunotargets Ther*. 2019;8:29–41. doi:10.2147/ITT.S219867
17. Zhou J, Wang G, Chen Y, et al. Immunogenic cell death in cancer therapy: present and emerging inducers. *J Cell Mol Med*. 2019;23(8):4854–4865. doi:10.1111/jcmm.14356
18. Zou Z, Zhao M, Yang Y, et al. The role of pyroptosis in hepatocellular carcinoma. *Cell Oncol*. 2023;46(4):811–823. doi:10.1007/s13402-023-00787-9
19. Calixto OJ, Meneses-Toro MA, Vera-Parra EC, et al. Posttranslational modifications in psoriatic arthritis: a systematic literature review. *Autoimmun Rev*. 2023;22:103393. doi:10.1016/j.autrev.2023.103393
20. Hsu WJ, Chiang MC, Chao YC, et al. Arginine methylation of DDX3 by PRMT1 mediates mitochondrial homeostasis to promote breast cancer metastasis. *Cancer Res*. 2023;16. doi:10.1158/0008-5472.CAN-23-3829
21. Jing L, Xia B, Chen C, et al. PRMT1 mediated methylation of cGAS suppresses anti-tumor immunity. *Nat Commun*. 2023;14(1):2806. doi:10.1038/s41467-023-38443-3
22. Kwontae Y, Lingfei W, ChihHung C, et al. QRICH1 dictates the outcome of ER stress through transcriptional control of proteostasis. *Science*. 2021;371(6524).
23. Jie H, Rui Z, Xinping W, et al. Active polypeptide MDANP protect against necrotizing enterocolitis (NEC) by regulating the PERK-eIF2α-QRICH1 axis. *Sci Rep*. 2023;13(1):22912. doi:10.1038/s41598-023-44194-4
24. Wang J. To study the expression and regulatory mechanism of QRICH1 in arsenic induced apoptosis of hepatoma cells[D]. Guizhou Medical University; 2023. doi:10.27045/d.cnki.ggyyc.2023.000147
25. Zhang X, Hu B, Sun YF, et al. Arsenic trioxide induces differentiation of cancer stem cells in hepatocellular carcinoma through inhibition of LIF/JAK1/STAT3 and NF-kB signaling pathways synergistically. *Clin Transl Med*. 2021;11:e335. doi:10.1002/ctm2.335
26. Cui Z, Zhang Y, Xia K, et al. Nanodiamond autophagy inhibitor allosterically improves the arsenical-based therapy of solid tumors. *Nat Commun*. 2018;9:4347. doi:10.1038/s41467-018-06749-2
27. Xia Y, Liu X, Liu B, et al. Enhanced antitumor activity of combined megestrol acetate and arsenic trioxide treatment in liver cancer cells. *Exp Ther Med*. 2018;15:4047–4055. doi:10.3892/etm.2018.5905
28. D DH, Mencin A, Gwak G, et al. Promotion of hepatocellular carcinoma by the intestinal microbiota and TLR4. *Cancer Cell*. 2012;21(4):504–516. doi:10.1016/j.ccr.2012.02.007
29. S R, M DK, W SN, et al. Cancer statistics, 2023. *Ca a Cancer J Clin*. 2023;73(1):17–48. doi:10.3322/caac.21763
30. Forner A, Reig M, Bruix J. Hepatocellular carcinoma. *Lancet (London, England)*. 2018;391:1301–1314. doi:10.1016/S0140-6736(18)30010-2
31. Wang J, Liang S, Zhu D, et al. Valence-Change MnO2-coated arsenene nanosheets as a Pin1 Inhibitor for hepatocellular carcinoma treatment. *J Am Chem Soc*. 2024.
32. Xuhua D, Hao L, Pengfei C, et al. Transcatheter arterial chemoembolization using CalliSpheres beads loaded with arsenic trioxide for unresectable large or huge hepatocellular carcinoma: a prospective study. *Eur Radiol*. 2023;34(2):1258–1267. doi:10.1007/s00330-023-10097-1
33. Ruf B, Heinrich B, Greten TF. Immunobiology and immunotherapy of HCC: spotlight on innate and innate-like immune cells. *Cell mol Immunol*. 2020;18(1):112–127. doi:10.1038/s41423-020-00572-w
34. Sun L, Su Y, Jiao A, et al. T cells in health and disease. *Signal Transduct Target Ther*. 2023;8:235. doi:10.1038/s41392-023-01471-y
35. Liu YT, Sun ZJ. Turning cold tumors into hot tumors by improving T-cell infiltration. *Theranostics*. 2021;11:5365–86.42. doi:10.7150/thno.58390
36. Xu Z, Xu J, Sun S, et al. Mecheliolide elicits ROS-mediated ERS driven immunogenic cell death in hepatocellular carcinoma. *Redox Biol*. 2022;54(40):41. doi:10.1016/j.redox.2022.102351
37. Shalhout SZ, Miller DM, Emerick KS, et al. Therapy with oncolytic viruses: progress and challenges. *Nat Rev Clin Oncol*. 2023;20:160–177. doi:10.1038/s41571-022-00719-w
38. Chen J, Jin Z, Zhang S, et al. Arsenic trioxide elicits prophylactic and therapeutic immune responses against solid tumors by inducing necroptosis and ferroptosis. *Cell mol Immunol*. 2023;20:51–64. doi:10.1038/s41423-022-00956-0
39. Li X, Zheng J, Chen S, et al. Oleandrin, a cardiac glycoside, induces immunogenic cell death via the PERK/elF2alpha/ATF4/CHOP pathway in breast cancer. *Cell Death Dis*. 2021;12:314.44.
40. Oresta B, Pozzi C, Braga D, et al. Mitochondrial metabolic reprogramming controls the induction of immunogenic cell death and efficacy of chemotherapy in bladder cancer. *Sci Transl Med*. 2021;13:eaba6110.
41. Yu P, Zhang X, Liu N, et al. Pyroptosis: mechanisms and diseases. *Signal Transduct Target Ther*. 2021;6:128.8.
42. Rosenbaum SR, Wilski NA, Aplin AE. Fueling the fire: inflammatory forms of cell death and implications for Cancer Immunotherapy. *Cancer Discov*. 2021;11:266–81.9. doi:10.1158/2159-8290.CD-20-0805

43. Liu X, Xia S, Zhang Z, et al. Channelling inflammation: gasdermins in physiology and disease. *Nat Rev Drug Dis*. 2021;20:384–405. doi:10.1038/s41573-021-00154-z
44. Tan Y, Chen Q, Li X, et al. Pyroptosis: a new paradigm of cell death for Fighting against cancer. *J Exp Clin Cancer Res*. 2021;40:153.15. doi:10.1186/s13046-021-02101-7
45. Li LR, Chen L, Sun ZJ. Igniting hope: harnessing NLRP3 inflammasome-GSDMD-mediated pyroptosis for cancer immunotherapy. *Life Sci*. 2024;354:122951. doi:10.1016/j.lfs.2024.122951